

Spectroscopic properties of *N-n*-hexyltetrachlorophthalimide and supramolecular interactions in its crystals

Bogumił Brycki^a, Iwona Kowalczyk^{a,*}, Andrzej Zieliński^a,
Teresa Borowiak^b, Irena Wolska^b

^a Laboratory of Microbiocides Chemistry, Faculty of Chemistry, Adam Mickiewicz University, Grunwaldzka 6, 60-780 Poznań, Poland

^b Department of Crystallography, Faculty of Chemistry, Adam Mickiewicz University, Grunwaldzka 6, 60-780 Poznań, Poland

Received 6 February 2007; received in revised form 23 March 2007; accepted 26 March 2007

Available online 3 April 2007

Abstract

N-n-hexyltetrachlorophthalimide has been characterized by X-ray diffraction, FTIR, Raman and NMR spectroscopy. Also B3LYP and DFT calculations have been carried out. The optimized bond lengths, bond angles and torsion angles calculated by B3LYP/6-31G(d,p) approach have been compared with the X-ray data. The screening constants for ¹³C and ¹H atoms have been calculated by the GIAO/B3LYP/6-31G(d,p) approach and analyzed. Linear correlations between the experimental ¹H and ¹³C chemical shifts and the computed screening constants confirm the optimized geometry. The supramolecular structure is organized into hydrophilic and hydrophobic segments. The tetrachlorophthalimide moieties of the hydrophilic segments form infinite chains *via* halogen bonds C=O...Cl. These bonds as well as weak intermolecular hydrogen bonds C—H...O contribute to the parallel orientation of the chains and to the stabilization of their flat conformation. The intermolecular Cl...Cl interactions stabilize the organization of the hydrophilic segments.

© 2007 Elsevier B.V. All rights reserved.

Keywords: *N-n*-Hexyltetrachlorophthalimide; X-ray diffraction; Supramolecular structure; Intermolecular halogen bond; DFT calculations; FTIR; Raman and NMR spectra

1. Introduction

The phthaloyl and tetrachlorophthaloyl groups are important pharmacophores [1]. Tetrachlorophthalimide derivatives are good α -glucosidase inhibitors, decreasing glucose level in blood by delaying digestion of poly- and oligosaccharides to absorbable monosaccharides. Due to that tetrachlorophthalimides can be potentially valuable for treatment of diabetes, hyperlipoteinemia, and obesity [2,3]. Some of tetrachlorophthalimide derivatives show cytotoxicity and antimicrobial activity, especially anti-human immunodeficiency virus (HIV) activity. This activity is thought to arise because of the ability of tetrachlorophthalimide derivatives to inhibit trimming glucosidases involved

in the biosynthesis of the N-linked oligosaccharides on the envelope glycoprotein [1]. *N-n*-Hexyltetrachlorophthalimide is one of a series of *N-n*-alkyltetrachlorophthalimides investigated in our laboratory in order to better understand the mechanism of their biocidal activity against bacteria and fungi. These compounds will be used as co-microbiocides with another group of antimicrobial agents to avoid the increase of resistance of microorganisms on the biocides applied. Structure and activity relationship studies on *N-n*-alkyltetrachlorophthalimide derivatives indicated that the hydrophobic groups at the N atom are of crucial meaning [4,5].

In this paper the X-ray structure as well as results on B3LYP calculations, FTIR, Raman and NMR spectroscopy of *N-n*-hexyltetrachlorophthalimide [hereafter **1**] are presented. The another aspect of our interest in tetrachlorophthalimides are their supramolecular structures where in

* Corresponding author. Tel.: +48 61 829 1306; fax: +48 61 865 8008.
E-mail address: ikow@amu.edu.pl (I. Kowalczyk).

the absence of strong hydrogen bond donors and/or acceptors a significant role in stabilizing the crystal packing play the other weak intermolecular forces.

2. Experimental

2.1. Synthesis

A mixture of equimolar amounts of tetrachlorophthalic anhydride and amine in toluene was heated under reflux for 20 h. After this time the solution was removed under reduced pressure. The residue was crystallized from hexane and dried under reduced pressure. Yield 84%, m.p. 145–146 °C. Analysis: found (calc) %C 45.5 (45.5); %H 4.0 (3.6); %N 3.8 (3.8).

2.2. Instrumentation

Crystals suitable for X-ray analysis were grown by slow evaporation from hexane solution. All details of the measurements, crystal data and structure refinement are given in Table 1. The data were collected on an Oxford Diffraction KM4CCD diffractometer [6] at 180 K (a phase transition at 156 K), using graphite-monochromated MoK α radiation. A total of 1072 frames were measured in six separate runs. The ω -scan was used with a step of 0.75°, two reference frames were measured after every 50 frames, they did not show any systematic changes either in peak posi-

tions or in their intensities. The unit cell parameters were determined by least-squares treatment of setting angles of 3855 highest-intensity reflections chosen from the whole experiment. Intensity data were corrected for the Lorentz and polarization effects [7]. The structure was solved by direct methods with the SHELXS97 program [8] and refined by the full-matrix least-squares method with the SHELXL97 program [9]. Six reflections were excluded from the reflection file due to their large ($|F_o|^2 - |F_c|^2$) differences. The function $\sum w(|F_o|^2 - |F_c|^2)^2$ was minimized with $w^{-1} = [\sigma^2(F_o)^2 + (0.0251P)^2 + 3.2952P]$, where $P = (F_o^2 + 2F_c^2)/3$. All non-hydrogen atoms were refined with anisotropic thermal parameters. The coordinates of the hydrogen atoms were calculated in idealized positions and refined as a riding model with their thermal parameters calculated as 1.2 (1.5 for methyl group) times U_{eq} of the respective carrier carbon atom.

The NMR spectra in CDCl $_3$ were measured for **1** with a Varian Gemini 300VT spectrometer, operating at 300.07 and 75.46 Hz for ^1H and ^{13}C , respectively. Infrared spectra were recorded in the KBr pellets using a FTIR Bruker IFS 113v spectrometer which was evacuated to avoid water absorption. The Raman spectrum was recorded on a Bruker IFS 66 spectrometer equipped with an FRA 106 Raman module operating at the 1064 nm exciting line of an Nd:YAG laser.

The calculations were performed using the GAUSSIAN 03 program package [10] at the B3LYP [10,11] levels of theory with the 6-31G(d,p) basis set [12]. The NMR isotropic shielding constants were calculated using the standard GIAO (Gauge-Independent Atomic Orbital) approach [10–13] of GAUSSIAN 03 program package [14].

CCDC 635823 for **1** contains the supplementary crystallographic data for this paper. These data can be obtained free of charge via www.ccdc.cam.ac.uk/data_request/cif, or by emailing data_request@ccdc.cam.ac.uk, or by contacting The Cambridge Crystallographic Data Centre, 12, Union Road, Cambridge CB2 1EZ, UK; fax: +44 1223 336033.

3. Results and discussion

3.1. The crystal structure of **1**

A view of the molecular structure together with the atom numbering scheme is shown in Fig. 1. The phthalimide moiety is approximately planar, the bond lengths and angles are comparable to those reported in the literature [15–19].

The supramolecular structure of **1** is particularly interesting when compared with that of the other derivative, *N*-*n*-butyltetrachlorophthalimide [hereafter (**2**)], [19]. The both molecules differ by two CH $_2$ groups in the substituent at N(1) and this steric factor causes substantial differences in the modes of packing. The crystal structure of **1** consists of hydrophobic and hydrophilic segments (Fig. 2) and in each of them the consecutive inversion centers connect

Table 1
Crystal data, data collection and structure refinement for **1**

| | |
|---|---|
| Empirical formula | C $_{14}$ H $_{13}$ Cl $_4$ NO $_2$ |
| Formula weight | 369.05 |
| <i>T</i> (K) | 180(2) |
| Wavelength (Å) | 0.71073 |
| Crystal system, space group | Triclinic, $P\bar{1}$ |
| Unit cell dimensions | |
| <i>a</i> (Å) | 5.0009(4) |
| <i>b</i> (Å) | 6.1160(5) |
| <i>c</i> (Å) | 27.036(2) |
| α (°) | 87.974(6) |
| β (°) | 88.199(6) |
| γ (°) | 75.300(7) |
| Volume (Å 3) | 799.1(1) |
| <i>Z</i> , <i>D_x</i> (Mg/m 3) | 2, 1.534 |
| μ (mm $^{-1}$) | 0.742 |
| <i>F</i> (000) | 376 |
| θ Range for data collection (°) | 3.45–29.87 |
| <i>h</i> / <i>k</i> / <i>l</i> Range | −6 ≤ <i>h</i> ≤ 6 −8 ≤ <i>k</i> ≤ 8 −36 ≤ <i>l</i> ≤ 37 |
| Reflections | |
| Collected | 10,565 |
| Unique (<i>R_{int}</i>) | 3988 (0.039) |
| Observed (<i>I</i> > 2 σ (<i>I</i>)) | 3421 |
| Data/restraints/parameters | 3988/0/190 |
| Goodness-of-fit on <i>F</i> 2 | 1.053 |
| <i>R</i> (<i>F</i>) (<i>I</i> > 2 σ (<i>I</i>)) | 0.0643 |
| <i>wR</i> (<i>F</i> 2) (all data) | 0.1386 |
| Max/min. (e/Å 3) | 0.737/−0.503 |

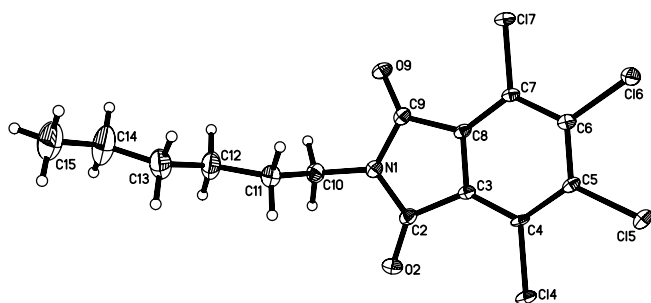


Fig. 1. A view of the molecule of **1**. Displacement ellipsoids are drawn at the 30% probability level and H atoms are depicted as spheres of arbitrary radii.

either the hydrophobic or the hydrophilic molecular fragments. If the main driving forces for the supramolecular structure formation for (**2**) are the $\text{C}-\text{Cl}\cdots\text{O}$, $\text{C}-\text{Cl}\cdots\text{Cl}-\text{C}$ and $\text{C}^{\delta+}\cdots\text{Cl}^{\delta-}$ intermolecular interactions, in **1** the diversity of interactions in the hydrophilic segment is higher and encompasses also the $\text{C}-\text{H}\cdots\text{O}$ weak hydrogen bonds. Thus, in **1** the hydrophilic segment is organized into two blocks of infinite chains (Fig. 2) which expand in the [110] direction (Figs. 2 and 3). The tetrachlorophthalimide moieties of each chain are coplanar (Fig. 4). Only one carbonyl group of the phthalimide moiety participates in the chain formation *via* a halogen bond $\text{C9}=\text{O9}\cdots\text{Cl4}-\text{C4}$ (Table 2, Figs. 3 and 4). The second carbonyl group, $\text{C2}=\text{O2}$ is involved in a bifurcated weak hydrogen bond $\text{C}-\text{H}\cdots\text{O}$ to the *n*-hexyl substituent which belongs to a molecule from the other molecular chain (Table 3 and Fig. 4). These bonds fulfill two functions: they contribute to the parallel orientation of chains and stabilize their flat conformation. The *n*-hexyl substituents of one block are oriented in the same direction like antennas being almost perpendicular to the phthalimide planes [the torsion angle $\text{C}(9)-\text{N}(1)-\text{C}(10)-\text{C}(11)$ is $-92.5(4)^\circ$ in **1**, the same angle in (**2**) is $-73.3(2)^\circ$). Molecules of two parallel chains are stacked with no overlap, the molecules of one chain are positioned over gaps of the other one (Fig. 4) in a consequence of electrostatic interactions $\text{C}(5)^{\delta+}\cdots\text{Cl}(7)^{\delta-}$ and $\text{C}(8)^{\delta+}\cdots\text{Cl}(4)^{\delta-}$, the both distances are shorter than the sum of the respective van der Waals radii and are equal

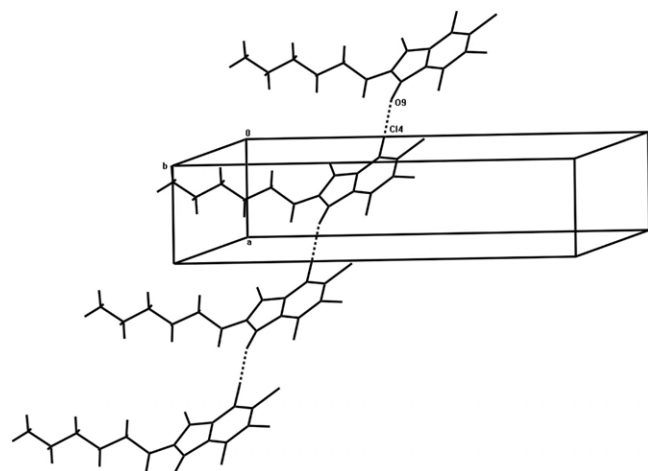


Fig. 3. One molecular chain which expands in the [110] direction.

to 3.380(3) and 3.421(3) Å, respectively. The hydrophilic blocks are joined *via* $\text{Cl}\cdots\text{Cl}$ interactions (Table 2, Fig. 5) [20].

3.2. B3LYP calculations

The optimized geometry parameters were computed by using the B3LYP and compared with the X-ray diffraction data in Table 4. The experimental and calculated bond lengths and bond angles are comparable in the most cases.

Some discrepancies in the values of torsion angles between the X-ray and theoretical data concern mainly the *n*-hexyl substituent and are caused by the packing forces.

3.3. FTIR and Raman spectra

Room-temperature solid-state FTIR and Raman spectra of **1** are shown in Fig. 6. The observed and calculated harmonic frequencies and their tentative assignments are listed in Table 5. These assignments are partly based on the calculated spectrum of *N*-tetrachlorophthalimide [21].

In the FTIR spectra of *N*-*n*-hexyltetrachlorophthalimide the stretching vibrations νCH_2 and νCH_3 groups are

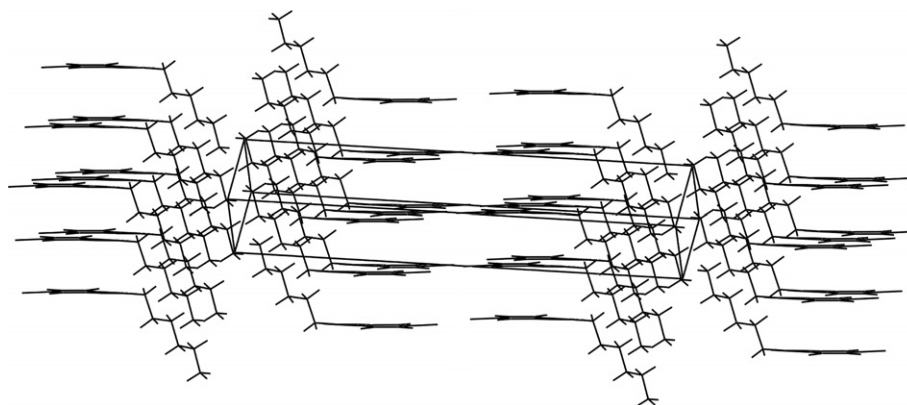


Fig. 2. The supramolecular structure of **1**. Hydrophilic and hydrophobic segments have been shown.

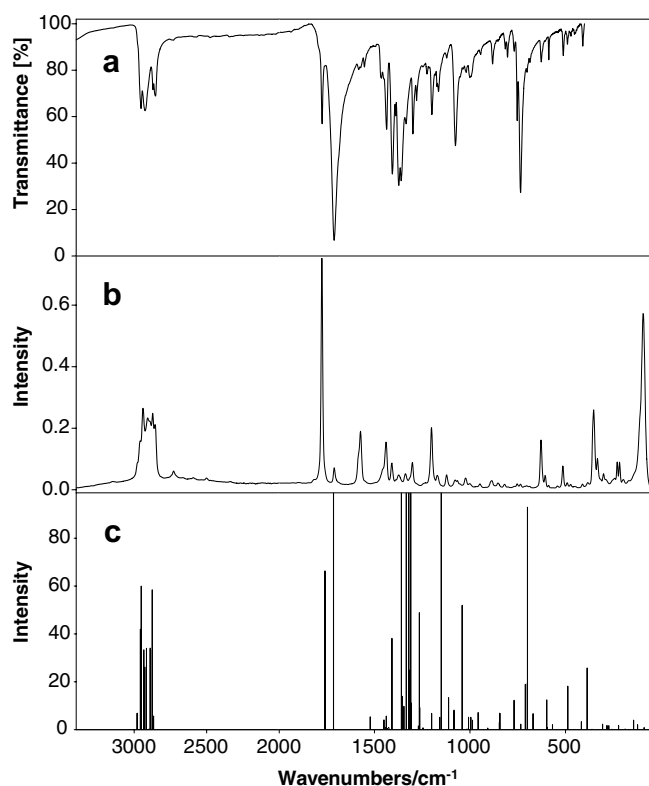


Fig. 6. Spectra of *N-n*-hexyltetrachlorophthalimide **1**: (a) FTIR (KBr pellet) (b) Raman and (c) Calculated spectrum.

proton–proton connectivity is observed through the off-diagonal peaks in the counter plot. The relations between the experimental ^1H and ^{13}C chemical shifts (δ_{exp}) and the GIAO (Gauge-Independent Atomic Orbitals) isotropic magnetic shielding tensors (σ_{calc}) are shown in Fig. 7. Both correlations are linear, described by the relationship: $\delta_{\text{exp}} = a + b \cdot \sigma_{\text{calc}}$. The a and b parameters are given in Table 6. Usually, the correlation between the experimental chemical shifts and calculated isotropic screening constants are better for carbon-13 atoms than for protons [14].

The very good correlation coefficients ($r^2 = 0.9933$) for ^1H and ($r^2 = 0.9954$) for ^{13}C correlations confirm the optimized geometry of **1**.

4. Conclusions

The molecular and crystal structures of *N-n*-hexyltetrachlorophthalimide **1** have been determined by X-ray diffraction, FTIR, ^1H , ^{13}C NMR spectroscopies and by the B3LYP calculations.

The *n*-hexyl substituent of the title compound causes substantial differences in the supramolecular structure in comparison with that of *N-n*-butyltetrachlorophthalimide.

FTIR spectra are consistent with the observed structure in the crystal. The good correlations between the experimental ^{13}C and ^1H chemical shifts in CDCl_3 solution of **1** and GIAO/B3LYP/6-31G(d,p) calculated isotropic shield-

Table 5
Observed and calculated B3LYP/6-31G(d,p) vibrational frequencies, infrared intensities for **1**

| Raman | IR | IR(calc.) | INT | Proposed assignment |
|---------|---------|-----------|------|----------------------------------|
| 2958 m | 2952 m | 2952 | 60.0 | νCH_2 |
| 2939 m | 2925 m | 2933 | 33.4 | νCH_2 |
| 2906 m | | | | νCH_2 |
| 2892 m | | | | νCH_2 |
| 2872 m | 2870 m | 2889 | 34.1 | νCH_2 |
| 2855 m | 2852 m | 2876 | 58.5 | νCH_2 |
| 2728 vw | 2729 vw | 2866 | 5.7 | νCH_2 |
| 1775 vs | 1774 m | 1759 | 66.4 | $\nu_{\text{as}}\text{CO}$ |
| 1711 w | 1711 vs | 1715 | 463 | $\nu_{\text{s}}\text{CO}$ |
| 1573 m | 1582 w | 1522 | 5.4 | νCC |
| | 1513 vw | 1520 | 0.1 | νCC |
| | 1464 m | 1451 | 4.1 | νCC |
| | 1450 m | 1442 | 0.9 | $\beta_{\text{as}}\text{CH}_3$ |
| 1439 w | 1436 s | 1438 | 5.7 | βCC |
| 1409 w | 1406 s | 1409 | 38.2 | νCC |
| 1388 w | 1389 w | 1359 | 102 | νCN |
| 1373 w | 1372 s | 1356 | 14.0 | $\beta_{\text{s}}\text{CH}_3$ |
| | 1360 s | 1346 | 9.8 | $\nu\text{CC}, \beta\text{CH}_2$ |
| 1338 w | 1334 m | 1334 | 289 | βCH_2 |
| | 1311 | 1310 | 141 | βCH_2 |
| 1301 w | 1299 m | 1308 | 11.2 | νCC |
| | 1224 w | 1265 | 48.9 | νCC |
| | 1214 w | 1264 | 9.3 | νCC |
| 1201 m | 1199 m | 1201 | 6.8 | νCN |
| 1171 w | 1181 w | 1158 | 5.2 | νCN |
| | 1172 w | 1150 | 155 | νCN |
| 1122 w | 1165 w | 1112 | 13.4 | γCH_2 |
| 1078 vw | 1076 m | 1084 | 8.2 | γCH_2 |
| 1066 vw | 1051 w | 1041 | 52.0 | γCH_2 |
| | 1037 w | 1016 | 0.3 | βCH_2 |
| 1023 vw | 1019 w | 1008 | 5.2 | βCCC |
| 1001 vw | 994 w | 996 | 5.2 | βCCC |
| 947 vw | 943 vw | 958 | 7.2 | βCO |
| 886 vw | 882 w | 907 | 0.7 | γCH_2 |
| 854 vw | 867 vw | 858 | 0.1 | γCH_2 |
| 819 vw | 815 w | 844 | 6.9 | βCCC |
| | 803 w | 770 | 12.3 | βCCC |
| 765 vw | 768 w | 734 | 2.3 | τring |
| 752 vw | 752 m | 711 | 19.0 | βCCC |
| 735 vw | 735 s | 705 | 0.1 | νCCl |
| 702 vw | 702 w | 700 | 19.3 | βCCC |
| 687 vw | 686 w | 699 | 93.0 | νCCl |
| 628 m | 627 w | 670 | 6.7 | βring |
| 588 vw | 587 w | 599 | 12.5 | βNCC |
| 513 w | 511 w | 568 | 2.1 | βCCC |
| 491 vw | 490 w | 515 | 0.1 | τring |
| 472 vw | 471 w | 488 | 18.2 | τring |
| 411 vw | 409 w | 417 | 3.4 | γCCC |
| 383 vw | | 386 | 25.8 | Lattice mode |
| 352 m | | 361 | 0.2 | νCCl |
| 332 w | | 332 | 0.1 | Lattice mode |
| 301 vw | | 306 | 2.3 | Lattice mode |
| 243 w | | 257 | 0.2 | Lattice mode |
| 229 w | | 222 | 1.8 | Lattice mode |
| 197 vw | | 188 | 0.3 | Lattice mode |
| 93 s | | 88.4 | 0.9 | Lattice mode |

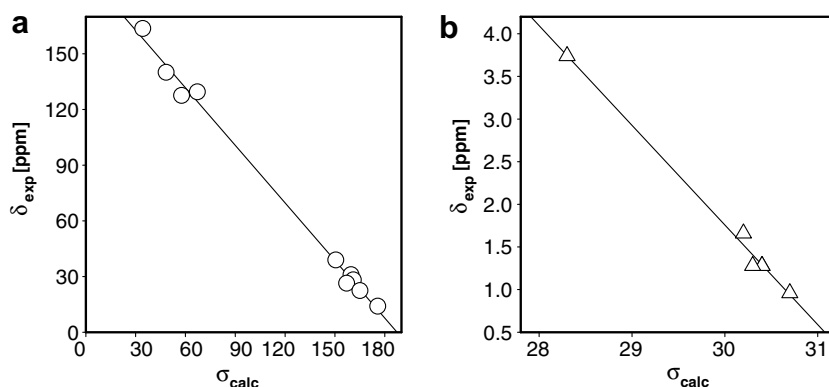
The abbreviations are: s: strong, m: medium, w: weak, vw: very weak, ν : stretching, β : in plane bending, δ : deformation, γ : out of plane bending and τ : twisting.

ing tensors ($\delta_{\text{exp}} = a + b \cdot \sigma_{\text{calc}}$) have confirmed the optimized geometry of **1**.

Table 6

Chemical shifts (δ , ppm) in CD₃Cl and calculating GIAO nuclear magnetic shielding tensors (σ_{calc}) for *N-n*-hexyltetrachlorophthalimide

| | $\delta_{\text{exp.}}$ | δ_{calc} | σ_{calc} | | $\delta_{\text{exp.}}$ | δ_{calc} | σ_{calc} |
|----------|------------------------|------------------------|------------------------|--------|------------------------|------------------------|------------------------|
| C (2,9) | 163.6 | 158.4 | 34.2 | H (10) | 3.74 | 3.74 | 28.3 |
| C (3,8) | 129.5 | 124.4 | 67.1 | H (11) | 1.66 | 1.53 | 30.2 |
| C (4,7) | 127.6 | 134.2 | 57.6 | H (12) | 1.28 | 1.29 | 30.4 |
| C (5,6) | 140.0 | 143.8 | 48.3 | H (13) | 1.28 | 1.29 | 30.4 |
| C (10) | 38.9 | 38.1 | 150.5 | H (14) | 1.28 | 1.41 | 30.3 |
| C (11) | 31.2 | 28.7 | 159.6 | H (15) | 0.95 | 0.94 | 30.7 |
| C (12) | 28.2 | 27.3 | 161.0 | | | | |
| C (13) | 26.4 | 31.4 | 157.0 | | | | |
| C (14) | 22.4 | 23.2 | 165.0 | | | | |
| C (15) | 14.0 | 12.1 | 175.7 | | | | |
| <i>a</i> | | 193.7361 | | | | 36.7990 | |
| <i>b</i> | | −1.0338 | | | | −1.1680 | |

The predicted GIAO chemical shifts were computed from the linear equation $\delta_{\text{exp.}} = a + b \cdot \sigma_{\text{calc}}$ with *a* and *b* determined from the fit the experimental data.Fig. 7. The relationship (a) between the experimental ¹³C chemical shifts (δ) and the GIAO computed ¹³C screening constants (σ) and (b) between the experimental ¹H chemical shifts (δ) and the GIAO computed ¹H screening constants (σ).

Acknowledgement

This work was supported by the funds from Adam Mickiewicz University, Faculty of Chemistry.

References

- [1] Y. Hashimoto, Bioorg. Med. Chem. 10 (2002) 461.
- [2] S. Sou, S. Mayumi, H. Takahashi, R. Yamasaki, S. Kadoya, M. Sodeoka, Y. Hashimoto, Bioorg. Med. Chem. Lett. 10 (2000) 1081.
- [3] S. Adisakwattana, K. Sookkongware, S. Roengsumran, A. Petsom, N. Ngamrojanavanich, W. Chavasiri, S. Deesamer, S. Yibchok-anun, Bioorg. Med. Chem. Lett. 14 (2004) 2893.
- [4] H. Takahashi, S. Sou, R. Yamasaki, M. Sodeoka, Y. Hashimoto, Chem. Pharm. Bull. 48 (2000) 1494.
- [5] N. Puviarasan, V. Arjunan, S. Mohan, Turk. J. Chem. 26 (2002) 323.
- [6] Oxford Diffraction Poland, CrysAlisCCD, CCD data collection GUI, version 1.171, 2003.
- [7] Oxford Diffraction Poland, CrysAlisRed, CCD data reduction GUI, version 1.171, 2003.
- [8] G.M. Sheldrick, Acta Crystallogr. A 46 (1990) 467.
- [9] G.M. Sheldrick, SHELXL97, Program for the Refinement of Crystal Structures, University of Göttingen, Germany, 1997.
- [10] M.J. Frisch, G.W. Trucks, H.B. Schlegel, G.E. Scuseria, M.A. Robb, J.R. Cheeseman, J.A. Montgomery Jr., T. Vreven, K.N. Kudin, J.C. Burant, J.M. Millam, S.S. Iyengar, J. Tomasi, V. Barone, B. Mennucci, M. Cossi, G. Scalmani, N. Rega, G.A. Petersson, H. Nakatsuji, M. Hada, M. Ehara, K. Toyota, R. Fukuda, J. Hasegawa, M. Ishida, T. Nakajima, Y. Honda, O. Kitao, H. Nakai, M. Klene, X. Li, J.E. Knox, H.P. Hratchian, J.B. Cross, C. Adamo, J. Jaramillo, R. Gomperts, R.E. Stratmann, O. Yazyev, A.J. Austin, R. Cammi, C. Pomelli, J.W. Ochterski, P.Y. Ayala, K. Morokuma, G.A. Voth, P. Salvador, J.J. Dannenberg, V.G. Zakrzewski, S. Dapprich, A.D. Daniels, M.C. Strain, O. Farkas, D.K. Malick, A.D. Rabuck, K. Raghavachari, J.B. Foresman, J.V. Ortiz, Q. Cui, A.G. Baboul, S. Clifford, J. Cioslowski, B.B. Stefanov, G. Liu, A. Liashenko, P. Piskorz, I. Komaromi, R.L. Martin, D.J. Fox, T. Keith, M.A. Al-Laham, C.Y. Peng, A. Nanayakkara, M. Challacombe, P.M.W. Gill, B. Johnson, W. Chen, M.W. Wong, C. Go.
- [11] A.D. Becke, J. Chem. Phys. 98 (1993) 5648.
- [12] P.J. Stephens, F.J. Devlin, C.F. Chabalowski, M.J. Frisch, J. Phys. Chem. 98 (1994) 11623.
- [13] W.J. Hehre, L. Random, P.V.R. Schleyer, J.A. Pople, Ab Initio Molecular Orbital Theory, Wiley, New York, 1986.
- [14] B. Ośmiałowski, E. Kolehmainen, R. Gawinecki, Magn. Res. Chem. 39 (2001) 334 (and ref. cited therein).
- [15] S.W. Ng, Acta Crystallogr. C 48 (1992) 1694.
- [16] L.-S. Zhou, Y.-Q. Feng, B. Gao, D.-X. Shi, X.-F. Li, Acta Crystallogr. E 59 (2003) o1066.
- [17] X.-G. Liu, Y.-Q. Feng, P. Wu, X. Chen, F. Li, Acta Crystallogr. E 60 (2004) o2293.
- [18] X.-G. Liu, Y.-Q. Feng, W. Wang, Z.-P. Liang, Y. Yang, Acta Crystallogr. E 61 (2005) o1316.
- [19] T. Borowiak, I. Wolska, B. Brycki, A. Zieliński, I. Kowalczyk, J. Mol. Struct. 833 (2007) 197.
- [20] V.R. Pedireddi, D.S. Reddy, B.S. Goud, D.C. Craig, A.D. Rae, G.R. Desiraju, J. Chem. Soc. Perkin Trans. 2 (1994) 2353.
- [21] Y. Hase, J. Mol. Struct. 52 (1979) 163.
- [22] E. Tatsch, B. Schrader, J. Raman Spectrosc. 26 (1995) 467.